京都大学防災研究所年報　第51号B　平成 20 年 6 月
Annuals of Disas. Prev. Res. Inst., Kyoto Univ., No. 51 B, 2008

Analysis of Peak Streamflow Distributions Based on Neyman-Scott Synthetic Rainfall

Carlo MONDONEDO*, Yasuto TACHIKAWA*, and Kaoru TAKARA

* Department of Urban and Environmental Engineering, Kyoto University

Synopsis

Synthetic rainfall generated in point processes should have consistent extreme values to that of historical rainfall to yield useful information for decision making. This is crucial for determining the impact of severe storms in areas with limited rainfall and/or streamflow data. We demonstrate this by comparing two methods for evaluating design floods in the Kamo and Kamishiiba River Basins in Japan. One method is based on the Japan Ministry of Land, Infrastructure, Transport, and Tourism (MLIT) that does not involve synthetic rainfall generation. Another method is based on the synthetic rainfall from the Neyman-Scott clustered point process. The latter method is observed to be more rational due to its consideration of extreme value rainfall.

Keywords: Synthetic Rainfall, Synthetic Streamflow, Point Processes, Neyman-Scott model

1. Introduction

Streamflow is the ultimate effect of rainfall in a river basin and is the basis of design decisions so that a safe coexistence can be established between a river basin and its inhabitants. Unfortunately, some river basins that would be advantageous to involve in flood control have limited rainfall and/or streamflow data for effective analysis. Many techniques have been developed to simulate the eventual transformation of rainfall into streamflow, such as distributed hydrological modeling (Beven, 2002). The same is true for tools developed for synthetic rainfall generation, as in the Neyman-Scott clustered Poisson rectangular pulse rainfall model, or NSM (Rodriguez-Iturbe et al, 1987).

Past contributions in the development of the NSM were based on making the synthetic extreme rainfall more consistent to its historical counterpart (Cowpertwait, 1998). The authors have also contributed to this problem in what they refer to as the NSM Fano factor exponent, or FFE (see Sec. 2). Through making synthetic rainfall extremes consistent to historical counterparts, one may generate lengthy records sufficient for analysis in a manner that is sound, safe, economical and efficient. Only then can one base design flood evaluation issues on a synthetic technique such that the lack of historical information is no longer a hindering factor in the decision-making process.

We demonstrate the advantage of synthetic rainfall generation in evaluating design streamflow by comparing two associated methodologies. One method excluding synthetic rainfall generation is based on the Japan Ministry of Land, Infrastructure, Transport, and Tourism (MLIT). Another method is developed by the authors based on the NSM. Both methods involve distributed hydrological modeling based on Kyoto University's Object Oriented Hydrologic Modeling System (OHyMOS).

2. Methodology

2.1 The NSM and its governing equations

The NSM is a clustered Poisson point process (Sefozo, 1990) in which: a) storms arrive following a temporal Poisson process (mean recurrence rate λ), b) storms consist of a geometric random number of rain cells, no storm containing zero cells (mean cell number μ_c), c) each cell arrival relative to the storm arrival follows an exponential distribution (mean lag time 1/β), d) each cell duration follows an exponential duration (mean duration 1/η), and e) each cell intensity follows a two-parameter gamma distribution (shape parameter α and scale parameter θ). The superposition of these rain cell pulses in the rainfall intensity-time plane results in the target synthetic rainfall. Six parameters are therefore required to tune the NSM for a particular application.

The following T-duration aggregated moments were derived for parameter estimation in the NSM (Rodriguez-Iturbe et al., 1987 and Cowpertwait, 1998). We include the expression for the Fano factor exponent (FFE) of the NSM. This expression is based on the spread of a count point process in time based on the Peaks Over Threshold rainfall point process (see Appendix). The latter is defined here as rainfall that exceeds the minimum block maxima in a historical rainfall record. The typical historical rainfall record involved in our experiments is limited to those that are pooled by monthly blocks so that the threshold is a smallest monthly maximum value.

$$\mathbf{E}[\mathbf{Y}] = \frac{\lambda \mu_c \alpha \theta}{\eta} T \tag{1}$$

$$\mathbf{Var}[\mathbf{Y}] = \frac{4\lambda\mu_c(\alpha\theta)^2 A_1(T)}{\eta^3} + \frac{2\lambda\mu_c\alpha\theta^2(1+\alpha)(\mu_c-1)\left[\beta^3 A_1(T) - \eta^3 B_1(T)\right]}{\beta\eta^3(\beta^2-\eta^2)} \tag{2}$$

$$A_1(T) = \eta T - 1 + \exp(-\eta T)$$

$$B_1(T) = \beta T - 1 + \exp(-\beta T)$$

$$\mathbf{Cov}[\mathbf{Y}_T, \mathbf{Y}_{T+k}] = \frac{4\lambda\mu_c(\alpha\theta)^2 A_2(T,k)}{\eta^3} + \frac{2\lambda\mu_c\alpha\theta^2(1+\alpha)(\mu_c-1)\left[\beta^3 A_2(T,k) - \eta^3 B_2(T,k)\right]}{\beta\eta^3(\beta^2-\eta^2)} \tag{3}$$

$$A_2(T,k,\eta) = \frac{1}{2}(1-\eta T)^2 \exp[(-\eta T)(k-1)]$$

$$B_2(T,k,\beta) = \frac{1}{2}(1-\beta T)^2 \exp[(-\beta T)(k-1)]$$

$$\mathbf{Cor}[\mathbf{Y}_T, \mathbf{Y}_{T+k}] = \frac{\mathbf{Cov}[\mathbf{Y}_T, \mathbf{Y}_{T+k}]}{\mathbf{Var}[\mathbf{Y}]} \tag{4}$$

$$\mathrm{TCM}[\mathbf{Y}] = \frac{6\lambda\mu_c\mathbf{E}[I^3]\left(\eta T - 2 + \eta T e^{-\eta T} + 2e^{-\eta T}\right)}{\eta^4} + \frac{3\lambda\mathbf{E}[I]\mathbf{E}[I^2]\mathbf{E}\{C(C-1)\}f(\eta,\beta,T)}{\left[2\eta^4\beta(\beta^2-\eta^2)^2\right]} + \frac{\lambda(\mathbf{E}[I])^3\mathbf{E}\{C(C-1)(C-2)\}g(\eta,\beta,T)}{\left[2\eta^4\beta(\eta^2-\beta^2)(\eta-\beta)(2\beta+\eta)(2\eta+\beta)\right]} \tag{5}$$

$$\mathrm{E}[I] = \alpha\theta; \quad \mathrm{E}[I^2] = \alpha(1+\alpha)\theta^2; \quad \mathrm{E}[I^3] = \theta^3\frac{\Gamma(3+\alpha)}{\Gamma(\alpha)}$$

$$\mathbf{E}\{C(C-1)\} = 2\mu_c(\mu_c-1); \quad \mathbf{E}\{C(C-1)(C-2)\} = 6\mu_c(\mu_c-1)^2$$

$$\begin{aligned} f(\eta,\beta,T) = {} & -2\eta^3\beta^2 e^{-\eta T} - 2\eta^3\beta^2 e^{-\beta T} + \eta^2\beta^3 e^{-2\eta T} \\ & + 2\eta^4\beta e^{-\eta T} + 2\eta^3\beta^2 e^{-(\eta+\beta)T} - 2\eta^4\beta e^{-(\eta+\beta)T} - 8\eta^3\beta^3 T \\ & + 11\eta^2\beta^3 - 2\eta^4\beta + 2\eta^3\beta^2 + 4\eta\beta^5 T + 4\beta\eta^5 T - 7\beta^5 \\ & - 4\eta^5 + 8\beta^5 e^{-\eta T} - \beta^5 e^{-2\eta T} - 2T\eta^3\beta^3 e^{-\eta T} - 12\eta^2\beta^3 e^{-\eta T} \\ & + 2T\eta\beta^5 e^{-\eta T} + 4\eta^5 e^{-\beta T} \end{aligned}$$

$$\begin{aligned} g(\eta,\beta,T) = {} & 12\eta^5\beta e^{-\beta T} + 9\eta^4\beta^2 + 12\eta\beta^5 e^{-\eta T} + 9\eta^2\beta^4 \\ & + 12\eta^3\beta^3 e^{-(\eta+\beta)T} - \eta^2\beta^4 e^{-2\eta T} - 9\eta^5\beta - 12\eta^3\beta^3 e^{-\beta T} \\ & - 9\beta^5\eta - 3\eta\beta^5 e^{-2\eta T} - \eta^4\beta^2 e^{-2\beta T} - 12\eta^3\beta^3 e^{-\eta T} \\ & - 3\beta\eta^5 e^{-2\beta T} - 10\beta^4\eta^3 T + 6\beta^5\eta^2 T - 10\beta^3\eta^4 T \\ & + 4\beta^6\eta T - 8\beta^2\eta^4 e^{-\beta T} + 4T\eta^6\beta + 12\eta^3\beta^3 - 8\eta^2\beta^4 e^{-\eta T} \\ & - 6\eta^6 - 6\beta^6 - 2\eta^6 e^{-2\beta T} - 2\beta^6 e^{-2\eta T} + 8\beta^6 e^{-\eta T} \\ & + 8\eta^6 e^{-\beta T} + 6\beta^2\eta^5 T \end{aligned}$$

$$\xi_{Si} = \frac{\ln\left[\left|\frac{A_i}{C_i}\left\{\frac{1}{\beta}\left(\gamma + \ln\left[(\mu_c-1)\frac{\eta}{\eta-\beta}\right]\right)\right\}^{(B_i-1)} - 1\right|\right]}{\ln\left[\frac{1}{\beta}\left(\gamma + \ln\left[(\mu_c-1)\frac{\eta}{\eta-\beta}\right]\right)\right]} \tag{6}$$

where **E[Y]** is mean rainfall depth, **Var[Y]** is the rainfall depth variance, **Cov**[$\mathbf{Y}_T$,$\mathbf{Y}_{T+k}$] is the rainfall depth autocovariance at lag-k, **Cov**[$\mathbf{Y}_T$,$\mathbf{Y}_{T+k}$] is the rainfall depth autocorrelation at lag-k, TCM[**Y**] = third central moment (TCM) of rainfall depth, ξ_{Si} = Fano Factor exponent (POT rainfall point process), and γ is the Euler constant (0.577…). The derivation of the FFE (eq. (6)) is shown in the Appendix (the interested reader is referred to Mondonedo et al., 2008 for further details).

The parameter estimation of the NSM is based on the solution of the following objective function:

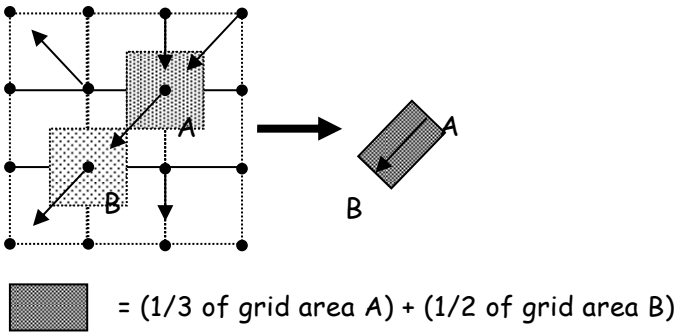

Fig. 1 Schematic diagram of the edge element used in the adopted Distributed Hydrologic Model (DHM).

$$O(\Omega) = \left(1 - \frac{NSM_i}{HIS_i}\right)^2 \quad (7)$$

where NSM_i pertains to the component expression listed in eqs. (1) – (6) while HIS_i pertains to the historical counterpart (see Appendix for historical counterpart of eq. (6)). Two combinations of components are used for parameter estimation for synthetic rainfall generation from the NSM. Scheme A is a configuration based on the TCM in which eq. (7) adopts the hourly mean, hourly variance, hourly autocorrelation at lag-1, hourly third central moment, 12-hourly autocorrelation at lag-1, 24-hourly variance, and 24-hourly autocorrelation at lag-1. Scheme B is essentially Scheme A, only that eq. (7) adopts the hourly FFE instead of the hourly TCM.

2.2 Description of adopted DHM

Two distributed hydrologic models (DHM) were developed from OHyMOS (Ichikawa, 2000). One model was developed for the Kamo river basin located in Kyoto Prefecture while another one was developed for Kamishiiba river basin in Miyazaki Prefectures in Japan. Both study areas were less than 300 Km^2 in size for which the use of a single rain gauge is justified. The river basins are represented as a collection of edge elements in each model. The edge element is essentially a connection of grid points determined to have the steepest gradient. Figure 1 shows three flow lines connected to grid point A while two flow lines connect to grid point B, indicating that 1/3 of the uniform grid area should be allotted to A while 1/2 the same area should be allocated to B to form edge AB. The width of this edge is determined by dividing the grid area by the distance between points A and B.

Rainfall-runoff conversion is implemented on elements such as AB in Fig. 1. This conversion follows a kinematic wave model following a function similar to a discharge-stage relationship (Tachikawa et al., 2007), shown in the succeeding equation:

$$q = \begin{cases} v_m d_m (h/d_m)^{\beta_m} & ; 0 \le h < d_m \\ v_m d_m + v_a (h - d_m) & ; d_m \le h < d_a \\ v_m d_m + v_a (h - d_m) + \alpha (h - d_a)^m & ; d_a \le h \end{cases} \quad (8)$$

and the continuity equation:

$$\frac{\partial q}{\partial x} + \frac{\partial h}{\partial t} = r \quad (9)$$

where q is discharge per unit width, h is flow depth, r is rainfall intensity, $v_m = k_m i$, $v_a = k_a i$, $k_m = k_a/\beta_m$, $\alpha = \sqrt{i}/n$, i is the gradient of the edge element, k_m is the saturated hydraulic conductivity of the capillary soil layer, k_a is the hydraulic conductivity of the non-capillary soil layer [m/s], n is the surface roughness coefficient [$m^{-1/3}s$], d_m is the capacity water depth for capillary soil layer [m], d_a is the capacity water depth including capillary and non-capillary soil layers [m] (see Fig. 2).

Parameters for these equations are assumed constant for all the edge elements in the river basin although internal systems are available for changing these parameters per sub-basin. These parameters were estimated in separate studies (Tachikawa et al., 2007 for Kamo and Lee et al., 2007 for Kamishiiba) and are shown in Table 1.

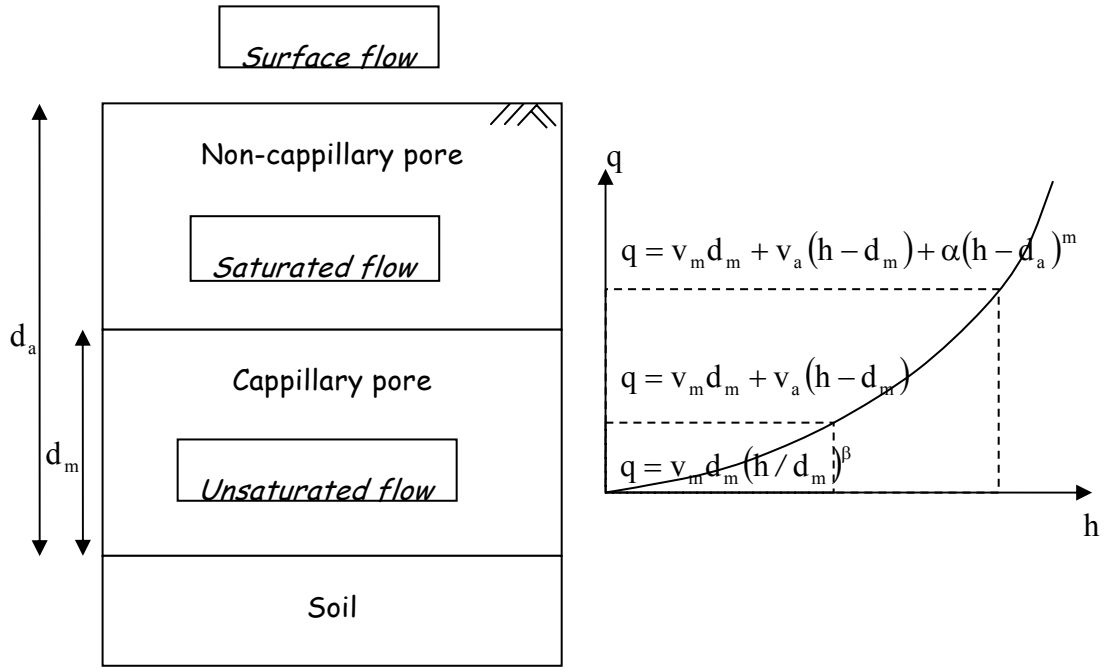

Fig. 2 (a)Model soil structure and (b) discharge-stage relationship adopted in river basin DHMs.

The simulations conducted with these tuned river basin models were set for monthly runs at 5 minute computation time with streamflow results displayed per hour.

3 Experimental Setup

Methods for calculating extreme floods are based on two procedures. One procedure is based on the Japan Ministry of Land, Infrastructure, Transport and Tourism (MLIT) while another is based on the NSM synthetic rainfall. For stationarity considerations, both methods are applied for historical rainfall pooled monthly during June, assumed to be stationary and representative of the rainy season in all study regions.

3.1 MLIT method

A procedure for estimating q-return period design floods from historical rainfall and streamflow simulation based on the Japan Ministry of Land, Infrastructure, Transport, and Tourism (MLIT, 2008) is designated here as M-I. This procedure starts with assigning a design duration from which the quantile rainfall for all simulations is based. For river basin areas such as Kamo and Kamishiiba, each less than 300 Km^2 in size, this duration is specified as 24 hours. The corresponding q-return period quantile rainfall depth is then calculated based on 24-hourly aggregated historical rainfall record. The MLIT then assigns a 24-hourly distribution to this total magnitude by searching through the historical records for the corresponding 24-hourly maximum rainfall per month. These maximum storms are then proportionately modified such that the total rainfall within the 24-hour period is the basis quantile rainfall.

The MLIT then runs each 24-hourly storm in an appropriate rainfall-runoff model to simulate

Table 1 Parameters of adopted Distributed Hydrological Models

River Basin	$n[m^{-1/3}s]$	$k_a[m/s]$	$d_a[m]$	$d_m[m]$	$\beta_m[-]$
Kamishiiba	0.3	0.010	0.55	0.45	0.65
Kamo	0.6	0.015	0.20	0.18	0.65

streamflow. There are thus as many resulting hydrographs from these simulations as there are historical rainfall records. Each hydrograph is then searched for its maximum value, yielding the estimate for the design flood, say S_{mq}. Consequently, M-I gives several estimates of the required q-return period design flood based on the S_{mq} of each simulated hydrograph.

3.2 Method based on NSM rainfall

A second streamflow generating procedure is designated here as M-II. We generate 100 synthetic records of the target month for our applications here where return periods are within the 100 year value. Each monthly record is then run through the appropriate river basin model for streamflow simulation.

The resulting hydrographs are checked for maximum streamflow, resulting in 100 values for flood frequency analysis. The required quantile event, say Q_{mq}, is then estimated from the cumulative distribution that best fits these empirical maxima (a log-normal distribution fitted by least squares is adopted for this purpose although other distributions may be used). Two further variants of this procedure correspond to the two NSM parameter estimation schemes of Sec. 2.1. M-IIA adopts NSM O(Ω) Scheme A while M-II adopts that of Scheme B for parameter generation.

4 Resulting Streamflow Estimates

Historical streamflow data was limited in this study. Each historical June rainfall record is also run through the appropriate DHM and is considered a suitable substitute for historical streamflow. Resulting quantile estimates from the synthetic streamflow and pseudo-historical counterparts shown here are limited to the hourly duration. Quantile streamflow are estimated for the 10-, 20-, 30-, 50-, and 100-year return periods.

4.1 Kamo river basin streamflow

The quantile-quantile (q-q) plot of Kamo pseudo-historical hourly streamflow maxima (Dis) appears in Figs. 3a-b. Each maximum streamflow value is given a plotting position pp proportionate to its rank in the overall record (pp=1/(i+1) in which i is rank). The log-normal distribution quantiles are used in this figure such that the independent variable (related to the event return period) corresponds to the inverse of the standard normal distribution (Gaussian distribution with zero mean and variance of unity) Φ^{-1} of pp while the dependent variable corresponds to the logarithm of Dis. The plot reflects a good correlation between this model and the pseudo-historical streamflow. Linear regression gives us the parameters for the fit of this log-normal model that leads to the 95% confidence bands.

We may then project the best fit line for the pseudo-historical streamflow (Fig. 3a) to extrapolate the trend at return periods 10-, 20-, 30-, 50-, and 100-years. We observe a tendency of M-I to give a wide range of estimates for these target quantile floods in Fig. 3a. In fact, the variation of M-I estimates becomes wider along with increasing return period. There is thus a pronounced ambiguity in the quantile estimates of M-I, making it disadvantageous despite its simple approach of using historical data alone. In other words, it would be difficult to depend on M-I to quantify the quantile events given that we cannot justify which among the multiple estimates is the most likely value.

This ambiguity does not appear in M-II, shown in Fig. 3b. Estimates appear to be quite consistent to the projections of pseudo-historical data. In particular, estimates generated from rainfall determined by parameters based on Scheme B appear to be the more rational estimate since this scheme includes POT rainfall maxima information in the FFE. The advantage of using M-II, which involves synthetic rainfall generation, is therefore its clearer and unambiguous estimates of the quantile events.

4.2 Kamishiiba river basin streamflow

Similar q-q plots based on Kamishiiba results appear in Figs. 4a-b. Not all quantile estimates generated from M-I are within reasonable proximity to what can be drawn from the pseudo-historical counterpart, as shown in the lower return periods (10-year and 20-year estimates), indicating poor performance. In fact, quantiles should be evaluated at higher return periods (i.e.: higher than

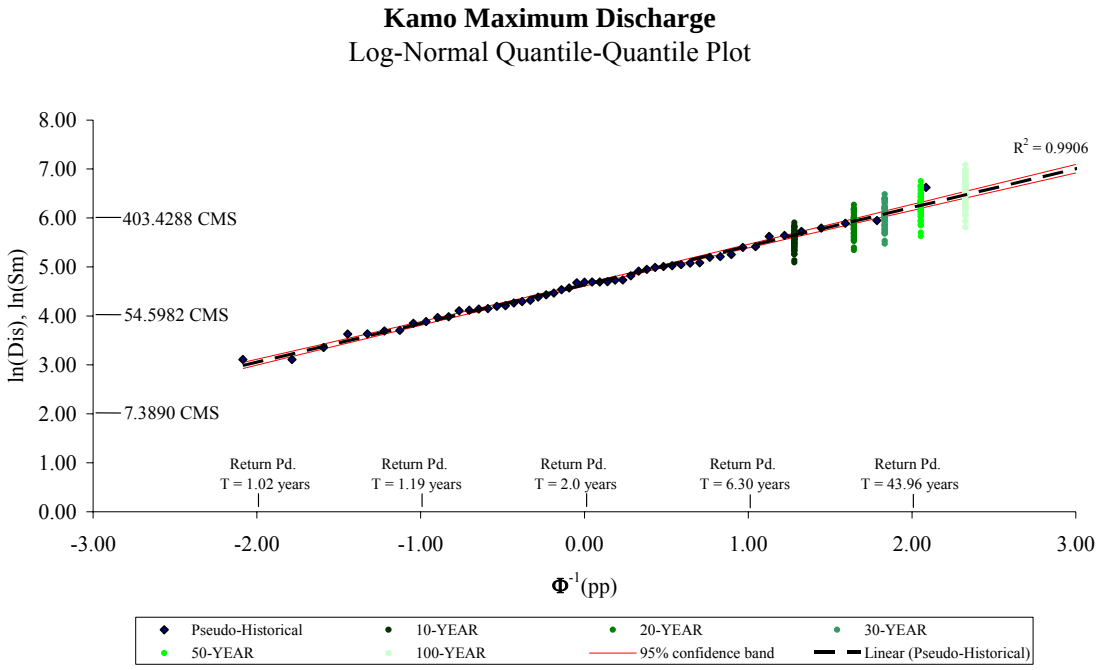

(a)

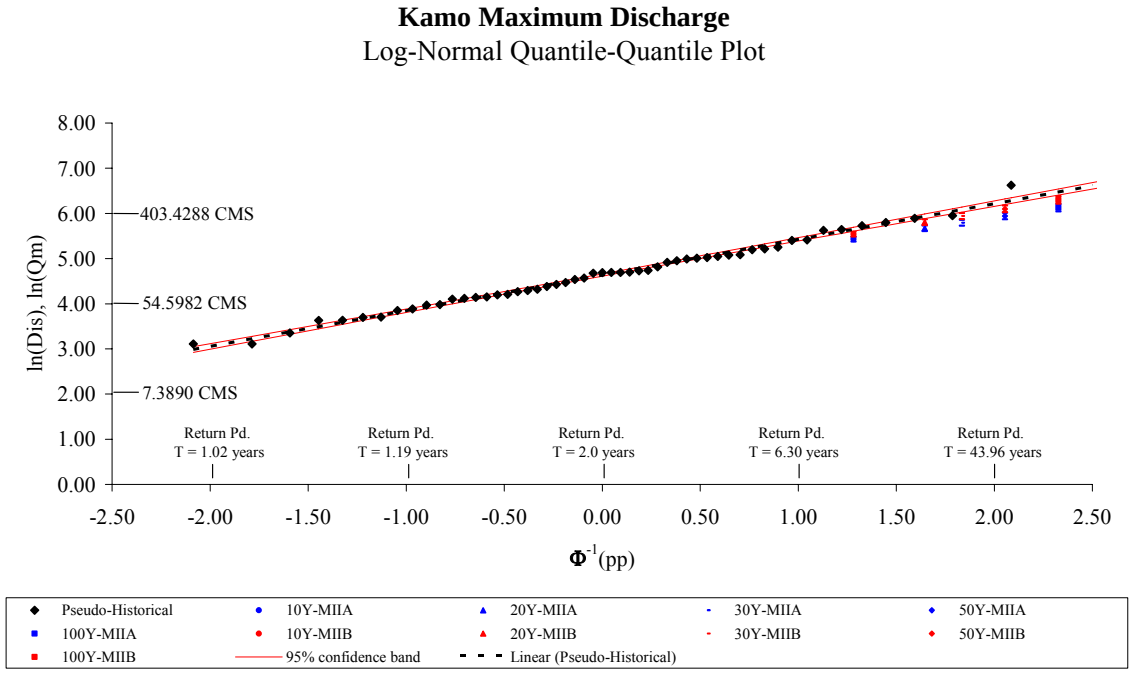

(b)

Fig. 3 Pseudo-historical streamflow block maxima from Kamo River with: (a) M-I synthetic quantiles and (b) M-II synthetic quantiles.

100 years) before the M-I method yields estimates with high variation that lie along the pseudo-historical 95% region. This however is not the ideal application since at times, one needs an estimate of lower return periods (i.e.: urban conditions/low priority flood protection works). The M-I scheme therefore generates poor estimates of the required quantiles in Kamishiiba River Basin.

On the other hand, Fig. 4b shows the same estimates generated from M-IIA and M-IIB. Most

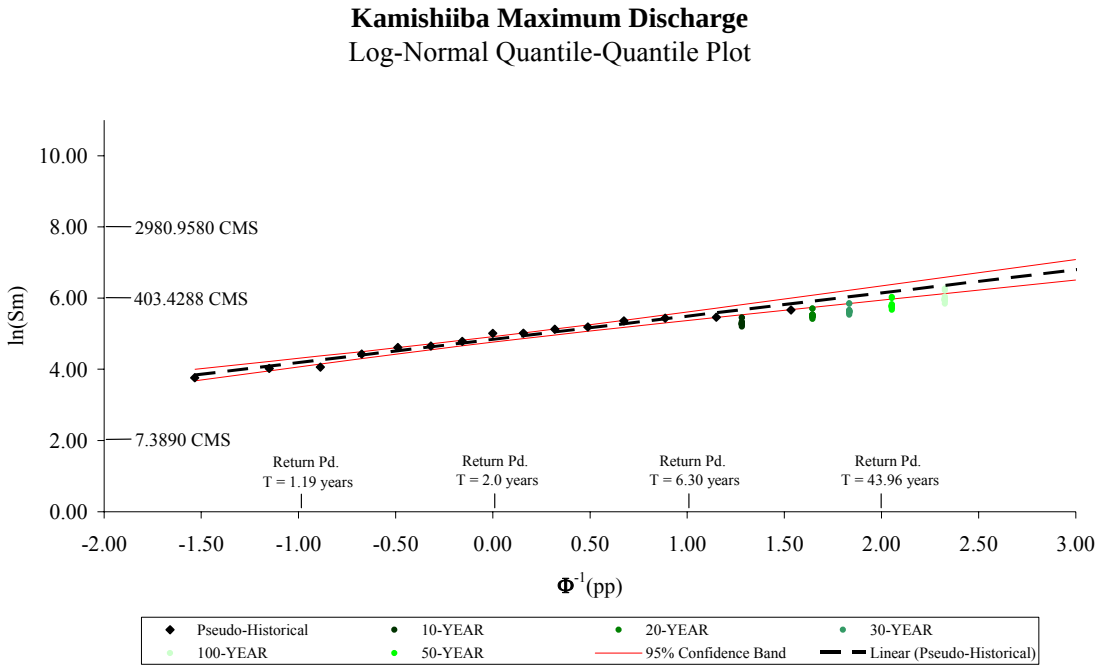

(a)

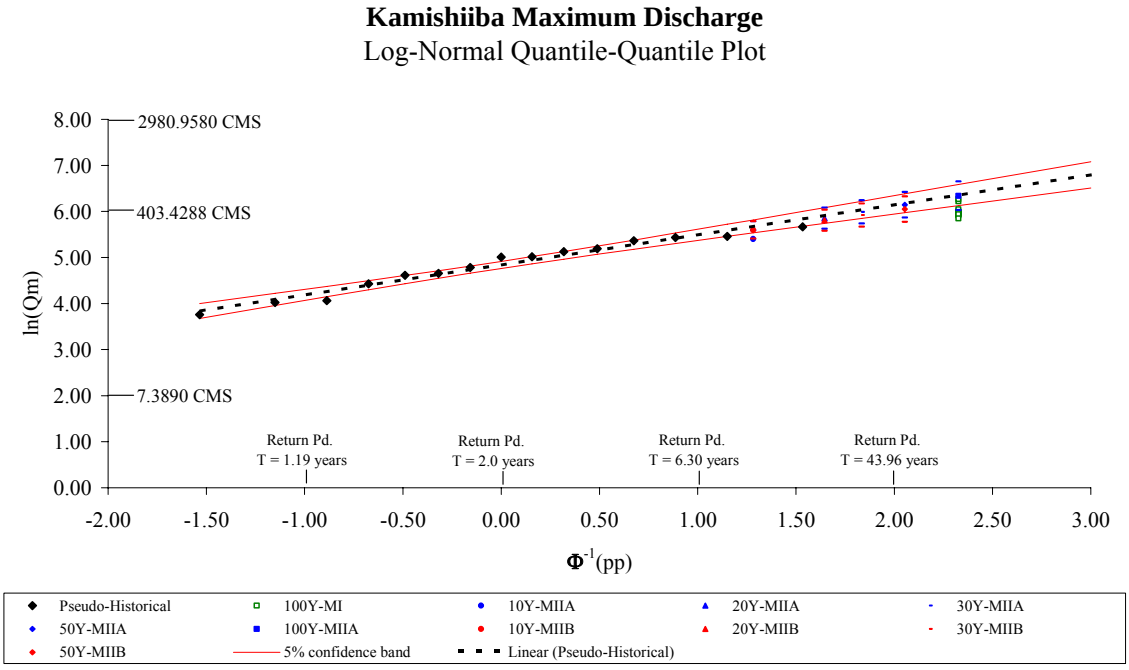

(b)

Fig. 4 Pseudo-historical streamflow block maxima from Kamishiiba River with: (a) M-I synthetic quantiles and (b) M-II synthetic quantiles.

quantile estimates are within the historical 95%region of historical quantiles, indicating better performance over the M-I estimates (of Fig. 4a). In fact, both schemes perform appreciably well given that both yield almost the same low return period estimates and gradually diverge at higher return periods within the 95% historical region. Therefore, either adopting M-IIA or M-IIB yields reasonable quantile estimates.

5 Conclusion

A comparison between several methods was conducted that led to the advantage of using synthetic rainfall in the estimation of critical streamflow in river basins with limited historical rainfall and/or streamflow data. Synthetic rainfall was based on the Neyman-Scott clustered Poisson rectangular pulse rainfall model (NSM). The streamflow generated from modeling historical rainfall through a distributed hydrological modeling (DHM) was assumed as an equivalent to historical streamflow (referred to as pseudo-historical streamflow).

Results indicate that an established method from the Japan Ministry of Land, Infrastructure, Transport, and Tourism (MLIT) for estimating design floods from historical rainfall have several limitations. Estimates from this method (for the Kamo River Basin in Kyoto) vary widely for any return period due the use of multiple design rainfall that are each plausible occurrences of the quantile event. In one application (Kamishiiba River Basin in Miyazaki), results were in gross error for low return periods. Though this method involved only historical rainfall, estimates were found to be generally unreliable.

Another method involving NSM synthetic rainfall generation appears to be more rational in both form and delivered results. There were no ambiguous or erroneous estimates from the results of this method. Estimates based on this method are therefore more reliable and recommendable than those of the former type.

References

MLIT (2008): 国土交通省 河川砂防技術基準, Japan Ministry of Land, Infrastructure, Transport, and Tourism, retrieved Feb. 26, 2008, < http://www.mlit.go.jp/river/shishin_guideline/gijutsu/gijutsukijunn/gijutsukijunn.pdf>.

Beven, K. (2002): Rainfall Runoff Modelling: The Primer, John Wiley & Sons Ltd, West Sussex.

Cowpertwait, P. S. P. (1991): Further developments of the Neyman-Scott clustered point process for modeling rainfall, Water Resources Research, Vol. 27, No. 7, pp. 1431-1438.

Cowpertwait, P. S. P. (1998): A Poisson-cluster model of rainfall: high-order moments and extreme values, Proceedings of the Royal Society of London A, Vol. 454, pp. 885-898.

Ichikawa Y., Tachikawa, Y., Takara, K., & Shiiba, M. (2000): Object-oriented Hydrological Modeling System, Proc. of Hydroinformatics 2000, [CD-ROM].

Lowen, S. B. and Teich, M. C. (1995): Estimation and simulation of fractal stochastic point processes, Fractals, Vol. 3, No. 1, pp. 183-210.

Lowen, S. B. and Teich, M. C. (2005): Fractal-based point processes, John Wiley & Sons, Inc., New Jersey.

Lee, G., Tachikawa, Y., and Takara, K. (2007): Identification of model structural stability through comparison of hydrologic models, Annual Journal of Hydraulic Engineering, JSCE, Vol. 51, pp. 49-54.

Mondonedo, C., Tachikawa, Y., and Takara K. (2008): POT normalized variance parameter search of the temporal Neyman-Scott rainfall model, Annual Journal of Hydraulic Engineering, JSCE, Vol. 52, pp. 97-102.

Rodriguez-Iturbe, I., Cox, D. R., and Isham, V. (1987): Some models for rainfall based on stochastic point processes, Proceedings of the Royal Society of London A, Vol. 410, pp. 269-288.

Sefozo, R. F. (1990): 'Point Processes' in Heyman, D. P. and Sobel, M. J. (eds.) Nemhauser, G. L. and Rinnooy Kan, A. H. G. (series eds.), Handbooks in Operations Research and Management Science Vol. 2: Stochastic Models, Elsevier Science Publishers, pp. 1-93.

Telesca, L., Lapenna, V., Scalcione, E., and Summa, D. (2007): Searching for time-scaling features in rainfall sequences, Chaos, Solitons, and Fractals, No. 32, pp. 35-41.

Tachikawa, Y., Takubo, Y. Sayama, T., and Takara, K. (2007): Large flood prediction in poorly gauged basins: the 2004 largest-ever flood in Fukui, Japan, Methodology in Hydrology (Proceedings of the Second International Symposium on Methodology in Hydrology held in Nanjing Chanina October-November 2005), IAHS Publ 311, pp. 18-24.

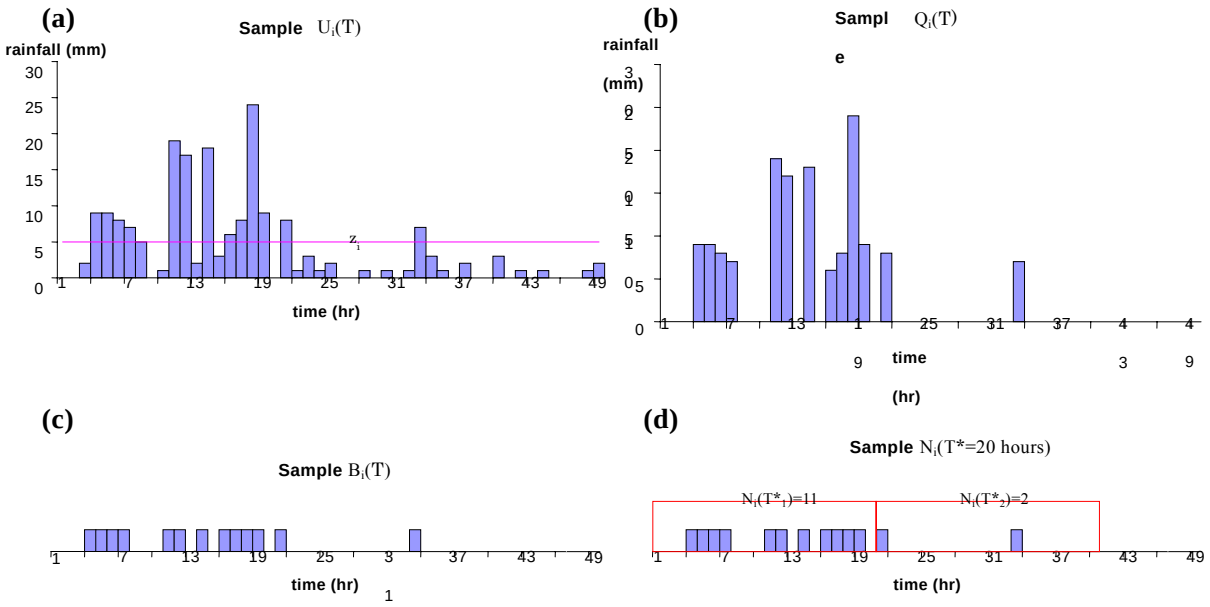

Fig. 5 Determining the Peaks Over Threshold (POT) rainfall point process and counting process $N_i(T^*)$. (a) sample rainfall $U_i(T)$ with previously determined threshold z_i, (b) POT rainfall $U_i(T)$ values greater than or equal to z_i (c) unit counts $B_i(T)$ assigned for each rainfall occurrence, (d) counting process $N_i(T^*)$.

Appendix

A thorough discussion regarding the NSM Fano factor exponent appears in Mondonedo et al., 2008. However, we present here a brief derivation of this expression. Figure 5 shows the construction of the special count process $N_i(T)$ to be used in determining the Fano factor $FF(T^*)$ at an arbitrary window T^*. With rainfall pooled for each month i (i=1: January, i=2: February, etc.), we define the process $U_i(T)$ (Fig. 5a), as the rainfall magnitude per fixed duration T (i.e.: T=1 hour in this study). For the M months in each $U_i(T)$, we determine the M monthly or block maxima $Z_i(T)$ and threshold value z_i, the minimum of $Z_i(T)$. We define the POT rainfall point process $Q_i(T)$ based on Eq. (10) (Fig. 5b):

$$Q_i(T)=\begin{cases} U_i(T); & U_i(T)\geq z_i \\ 0 \;\; ; & U_i(T)<z_i \end{cases} \qquad (10)$$

For each rainfall occurrence in $Q_i(T)$, we define the binary process $B_i(T)$ based on Eq.(11) (Fig. 5c). This process counts all durations of rainfall greater than or equal to the threshold z_i and serves as the basis for defining the Fano factor used here:

$$B_i(T)=\begin{cases} 1; & Q_i(T)>0 \\ 0; & Q_i(T)=0 \end{cases} \qquad (11)$$

Using adjacent windows of arbitrary value T^*, we define the count process $N_i(T^*)$, the sum of $B_i(T)$ within each segment T^* (Fig. 5d).

The Fano factor $FF(T^*)$ is defined as the ratio of variance of count $N_i(T^*)$ and mean of $N_i(T^*)$, or:

$$FF_i(T^*)=\frac{E\langle[N_i(T^*)]^2\rangle-E\langle N_i(T^*)\rangle^2}{E\langle N_i(T^*)\rangle} \qquad (12)$$

where:

$E\langle\ \rangle$ = operation to obtain expected value.

Based on data from independent studies, Lowen and Teich (1995, 2005) and Telesca et al. (2007) proposed the power law relationship of Eq. (13) to describe the scaling that occurs over several decadal values of T (Fig. 6):

$$FF(T^*)=1+\left(\frac{T^*}{T_0}\right)^{\xi} \qquad (13)$$

in which T^*_0 is the basic data duration (i.e.: $T^*_0 = 1$

hour here) and ξ is a fractal exponent (0≤ξ≥1). Strictly speaking, the rainfall data used by Telesca et al., 2007) were pooled yearly (z_i = 0) instead of $Q_i(T)$. It was assumed here that Eq. (7) is valid for $Q_i(T)$ throughout the small set of windows $T \in \mathcal{W}$ = {2, 10, 20, …, 100 hours} (Fig.6).

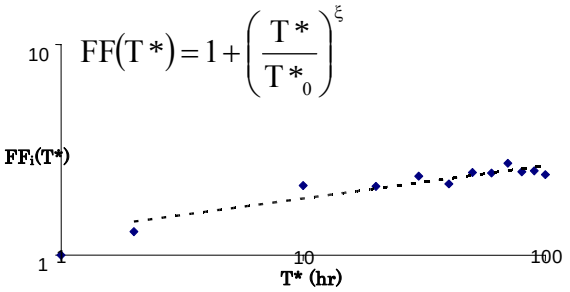

Fig. 6 Scaling in the counting process $N_i(T^*)$ obtained from Kamishiiba POT series $Q_i(t)$ in June.

Alternatively, within $\mathcal{W}$, the approximations for variance and mean of $N_i(T^*)$ are proposed here as Eqs. (14) and (15) such that the Fano factor can be independently estimated as Eq. (16).

$$\mathrm{Var}\langle N_i(T^*)\rangle = A_i T^{*B_i} \tag{14}$$

$$E\langle N_i(T^*)\rangle = C_i T^* \tag{15}$$

$$FF_i(T^*) \approx \frac{A_i}{C_i} T^{*B_i - 1} \tag{16}$$

After curve fitting operations for Eqs. (14) and (15) (i.e.: linear regression of historical $Q_i(T)$ for determining A_i, B_i, and C_i), Eq. (16) is used to explicitly determine $FF_{Hi}(T_{Mi})$, the Fano factor of the historical $Q_i(T)$ at window T* = mean storm duration T_{Mi} such that:

$$FF_{Hi}(T_{Mi}) \approx \frac{A_i}{C_i} T_{Mi}^{B_i - 1} \tag{17}$$

The relationship for the synthetic equivalent $FF_{Si}(T_{Mi})$ can be written explicitly using Eq. (13) such that:

$$FF_{Si}(T_{Mi}) = 1 + \left(\frac{T_{Mi}}{T_0}\right)^{\xi_{Si}} \tag{18}$$

For our purposes, an ideal simulation should yield synthetic rainfall with $Q_i(T)$ such that historical Fano factor $FF_{Hi}(T_{Mi})$ and synthetic Fano factor $FF_{Si}(T_{Mi})$ are equal, or based on Eqs. (16) and (18):

$$\frac{A_i}{C_i} T_{Mi}^{B_i - 1} = 1 + \left(\frac{T_{Mi}}{T_0}\right)^{\xi_{Si}} \tag{19}$$

Isolating the synthetic Fano factor exponent ξ_{Si} leads to an expression relating properties of the historical $Q_i(T)$ to the unknown mean duration T_{Mi}.

$$\xi_{Si} = \frac{\ln\left[\left[\frac{A_i}{C_i} T_{Mi}^{(B_i - 1)} - 1\right]\right]}{\ln[T_{Mi}] - \ln[T_0]} \tag{20}$$

Actual mean storm duration T_{Mi} was estimated here based on Cowpertwait's expression (1991) derived from the NSM parameters shown here as Eq. (21):

$$T_{Mi} = 1/\beta\left(\gamma + \ln\left[(\mu_c - 1)\frac{\eta}{\eta - \beta}\right]\right) \tag{21}$$

By substituting Eq. (21) for T_{Mi} in Eq. (20), a direct link between historical $Q_i(T)$ and the NSM parameters is established as Eq. (22).

$$\xi_{Si} = \frac{\ln\left[\left[\frac{A_i}{C_i}\left\{\frac{1}{\eta}\left(\gamma + \ln\left[(\mu_c - 1)\frac{\eta}{\eta - \beta}\right]\right)\right\}^{(B_i - 1)} - 1\right]\right]}{\ln\left[\frac{1}{\eta}\left(\gamma + \ln\left[(\mu_c - 1)\frac{\eta}{\eta - \beta}\right]\right)\right] - \ln[T_0]} \tag{22}$$

Moreover, with the historical exponent ξ_{Hi} estimable through curve fitting Eq. (13) to the historical $Q_i(T)$, it is now possible to include ξ_{Si}, the NSM Fano factor exponent, in the NSM parameter estimation (through objective function $O(\Omega)$).

ノイマンスコット型の降雨時系列発生モデルをもとにした洪水ピーク流量の分析

Carlo MONDONEDO*・立川康人*・宝　　馨

*京都大学大学院工学研究科　都市環境工学専攻

要　旨

降雨の極値特性を反映するような降雨時系列の発生手法は，河川計画において有用と考えられる。特に，降雨や河川流量のデータが不十分な地域において豪雨の影響を分析するためには，降雨の時系列発生手法は極めて重要なツールとなる。本研究では，鴨川流域と桂川流域において計画洪水を評価するために２つの方法を比較する。一つは，国土交通省が標準的な方法として用いている方法であり，もう一つは，ノイマンスコット型のクラスターポイントプロセスモデルによって発生させた降雨時系列を用いる方法である。後者の方法は，降雨の極値特性を考慮する過程において，より合理的な方法と考えられる。

キーワード: 発生させた降雨時系列，発生させた流量時系列，ポイントプロセス，ノイマン・スコットモデル